42.24, 37.49, 31.08, 29.91, 29.59, 27.15, 25.96, 25.24; LRMS (NH_3, rel intensity) 330 (M + 18, 40), 313 (M + 1, 39), 295 (19), 281 (81), 263 (46), 253 (13), 235 (48), 223 (63), 205 (67), 195 (41), 137 (21); HRMS (CI, NH_3) calcd for $C_{17}H_{29}O_5$ (M + H) 313.2015, found 313.2020.

Trioxane Ether 13d. An oven-dried 5-mL one-necked round-bottomed flask was charged with trioxane alcohol **3** (36.8 mg, 0.14 mmol), dry *N,N*-dimethylformamide (0.5 mL), and 4-(chloromethyl)-3,5-dimethylisoxazole (40 μL, 0.32 mmol) via a gas-tight syringe and cooled to 0 °C under argon atmosphere. This solution was treated with sodium hydride (60% dispersion on mineral oil, ca. 10 mg, 0.25 mmol). After being stirred for 10 min at 0 °C, the reaction mixture was slowly warmed to room temperature and stirred for 2 h. The usual workup furnished the corresponding trioxane ether **13d** (31.7 mg, 61%) as a colorless oil: FT-IR ($CHCl_3$, cm^{-1}) 1638; ^1H NMR ($CDCl_3$, 400 MHz) δ 5.13 (s, 1 H), 4.29 (d, *J* = 12.0 Hz, (1 H), 4.22 (d, *J* = 12.0 Hz, 1 H), 3.50–3.44 (m, 2 H), 3.48 (s, 3 H), 2.38 (s, 3 H), 2.38–2.27 (m, 1 H), 2.27 (s, 3 H), 2.27–2.19 (m, 1 H), 2.01 (ddd, *J* = 14.2, 5.0, 3.2 Hz, 1 H), 1.89–1.47 (m, 8 H), 1.38 (s, 3 H), 1.38–1.16 (m, 2 H); ^{13}C NMR ($CDCl_3$, 100 MHz) δ 167.07, 159.92, 111.24, 105.18, 100.20, 85.30, 66.04, 68.71, 61.16, 56.68, 48.59, 41.93, 37.47, 31.02, 29.73, 29.49, 27.10, 25.93, 25.21, 11.02, 10.09; LRMS (NH_3, rel intensity) 382 (M + 1, 11), 364 (3), 350 (6), 322 (100), 239 (9), 225 (18), 195 (78), 181 (31), 137 (15), 110 (36); HRMS (CI, NH_3) calcd for $C_{20}H_{32}NO_8$ (M + H) 382.2230, found 382.2224.

Trioxane Carboxylate Ester 14. An oven-dried 10-mL one-necked round-bottomed flask was charged with terephthaloyl chloride (95.7 mg, 0.5 mmol) and dry methylene chloride (1 mL) and cooled to 0 °C. To this solution was added triethylamine (200 μL, 1.4 mmol) via a gas-tight syringe. After the reaction mixture was slowly warmed to room temperature over 0.5 h and stirred for 0.5 h, it was treated with trioxane alcohol **3** (58.5 mg, 0.22 mmol) in methylene chloride (1 mL). This reaction mixture was stirred for 1 h and the solvent was removed at reduced pressure to yield a crude product which was directly separated by silica gel column chromatography to afford the corresponding pure bis-trioxane carboxylate ester **14** (51.8 mg, 71%) as a colorless oil: FT-IR (neat) 1720; ^1H NMR ($CDCl_3$, 400 MHz) δ 8.10 (s, 4 H), 5.21 (s, 2 H), 4.48–4.35 (m, 4 H), 3.53 (s, 6 H), 2.45–2.30 (m, 4 H), 2.06–2.00 (m, 2 H), 1.91–1.66 (m, 4 H), 1.65–1.50 (m, 14 H), 1.45–1.34 (m, 2 H), 1.39 (s, 6 H), 1.34–1.21 (m, 2 H); ^{13}C NMR ($CDCl_3$, 100 MHz) δ 166.85, 134.08, 129.55, 105.29, 100.11, 85.19, 64.38, 56.71, 48.56, 42.33, 37.48, 31.00, 29.43, 29.18, 27.10, 25.93, 25.18; LRMS (NH_3, rel intensity) 692 (M + 18, 9), 657 (1), 632 (11), 572 (64), 466 (11), 404 (12), 348 (22), 318 (17), 233 (16), 195 (100), 177 (11), 168 (24), 137 (14), 119 (35), 117 (23); HRMS (CI, NH_3) calcd for $C_{36}H_{54}NO_{12}$ (M + NH_4) 692.3646, found 692.3662.

Biology. Bulk drugs were dissolved in DMSO and 70% ethanol and diluted in culture medium (RPMI 1640) with 10% human plasma. Microtiter plates were prepared with 2-fold serial dilutions of the drugs over a concentration range of 0.062–256 ng/mL and the parasite suspension (at 0.5% parasitemia and a 1% hematocrit) were incubated at 37 °C in an air-tight plexiglass box which was flushed with 5% oxygen, 5% carbon dioxide, and 90% nitrogen. After 24 h of incubation, the cultures were labeled with [^3H]hypoxanthine and incubated for an additional 18–20 h. At that time particulate matter was harvested from each well by using an automated cell harvester (MACH II, TOMTEC, Orange, CT). [^3H]Hypoxanthine that was incorporated by the parasites in each well was then measured by scintillation spectrophotometry (LKB 1205 Betaplate, Wallac, Inc., Gaithersburg, MD). All tested drugs, as well as positive and negative controls were run in duplicate.

Acknowledgment. We thank the Environmental Health Sciences Center, School of Hygiene and Public Health, of The Johns Hopkins University for financial support of the chemistry program and Dr. N. Narashima Murthy and Professor Kenneth Karlin, of The Johns Hopkins University Chemistry Department, for the X-ray crystallography data on trioxane alcohol **3**. Financial support for culturing the malaria parasites and conducting drug assays was provided the UNDP/World Bank/WHO Special Programme for Research and Training in Tropical Diseases (TDR).

NMR Studies of an FK-506 Analog, [U-^{13}C]Ascomycin, Bound to FK-506-Binding Protein

Andrew M. Petros, Gerd Gemmecker, Placido Neri, Edward T. Olejniczak, David Nettesheim, Robert X. Xu, Earl G. Gubbins, Harriet Smith, and Stephen W. Fesik*

Pharmaceutical Discovery Division, Abbott Laboratories, Abbott Park, Illinois 60064. *Received January 29, 1992*

Multidimensional, heteronuclear NMR methods were used to determine the complete ^1H and ^{13}C resonance assignments for [U-^{13}C]ascomycin bound to recombinant FKBP, including stereospecific assignment of all 22 methylene protons. The conformation of ascomycin was then determined from an analysis of NOEs observed in a ^{13}C-edited 3D HMQC-NOESY spectrum of the [U-^{13}C]ascomycin/FKBP. This structure is found to be quite different from the solution structure of the two forms of uncomplexed FK-506. However, it is very similar to the X-ray crystal structure of FK-506 bound to FKBP, rms deviation = 0.56 Å. The methods used for resonance assignment and structure calculation are presented in detail. Furthermore, FKBP/ascomycin NOEs are reported which help define the structure of the ascomycin binding pocket. This structural information obtained in solution was compared to the recently described X-ray crystal structure of the FKBP/FK-506 complex.

Introduction

The FK-506-binding protein, FKBP, is an 11.8-kDa protein that catalyzes the interconversion of the cis and trans rotamers of peptidyl-prolyl amide bonds.[1,2] This rotamase activity is inhibited by the immunosuppressant FK-506, which binds tightly ($K_d \sim 0.4$ nM) to this small enzyme. However, the binding of FK-506 to FKBP, although necessary, is not a sufficient condition for immunosuppressive activity. Recent studies suggest that upon formation of the FK-506/FKBP complex immunosuppressive activity is mediated by binding to and inhibiting the activity of the calcium-dependent phosphatase, calcineurin.[3]

*To whom correspondence should be addressed.

(1) Siekierka, J. J.; Hung, S. H. Y.; Poe, M.; Lin, C. S.; Sigal, N. H. A cytosolic binding protein for the immunosuppressant FK-506 has peptidyl-proyl isomerase activity but is distinct from cyclophilin. *Nature* **1989**, *341*, 755–757.

(2) Harding, M. W.; Galat, A.; Uehling, D. E.; Schreiber, S. L. A receptor for the immunosuppressant FK-506 is a cis-trans peptidyl-proyl isomerase. *Nature* **1989**, *341*, 758–760.

0022-2623/92/1835-2467$03.00/0

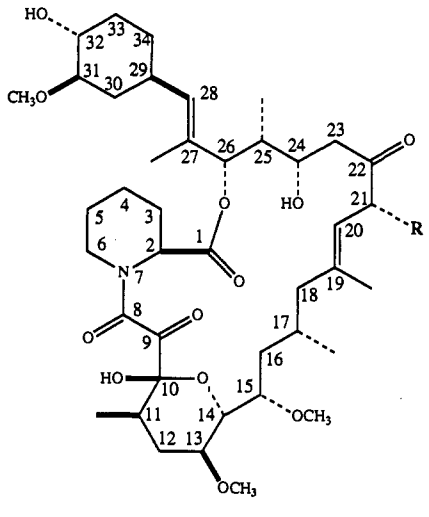

FK-506 R= $CH_2CH{=}CH_2$
Ascomycin R= CH_2CH_3
35 36

Figure 1. Structures of FK-506 and ascomycin.

In an attempt to provide structural information that may aid in the design of improved immunosuppressants, we have undertaken NMR studies of ascomycin (Figure 1)[4,5] and other analogs when bound to recombinant FKBP. In an initial communication,[6] we described the conformation of an FK-506 analog, [U-^{13}C]ascomycin, when bound to FKBP as determined by 3D heteronuclear NMR spectroscopy. Due to space limitations, we were unable to provide a complete description of the methods used to assign the ^{1}H and ^{13}C signals of the bound ligand or the experimental details of the structure calculations. These details are important for others interested in studying the conformation of enzyme-bound ligands. In this paper, we describe these procedures in detail. In addition, we compare the structure of ascomycin when bound to FKBP as determined by NMR to the recently described[7] X-ray structure of FK-506 bound to FKBP and to NMR structures of uncomplexed FK-506 determined in chloroform solution.[8,9] Finally, we have assigned several FKBP/ascomycin NOEs which define the ascomycin binding site, and we compare these results obtained in solution to those recently obtained for the FKBP/FK-506 complex by X-ray crystallography.[7]

Methods

Preparation of [U-^{13}C]Ascomycin. [U-^{13}C]Ascomycin was produced in a chemically defined fermentation medium. The nonorganic portion of the medium consisted of 0.5% $(NH_4)_2HPO_4$, 0.2% K_2HPO_4, 0.1% $MgSO_4{\cdot}7H_2O$, 0.04% $CaCl_2{\cdot}2H_2O$, 0.002% $FeSO_4{\cdot}7H_2O$, 0.001% $ZnSO_4{\cdot}7H_2O$, and 0.0005% $CoCl_2{\cdot}2H_2O$ in distilled water. The carbon source, uniformly ^{13}C-labeled glucose (fermentation grade, Martek Corp., Columbia, MD), was sterilized separately and added to the salt solution at 1%. Spores of *Streptomyces hygroscopicus* subsp. *ascomyceticus* UV125, a strain obtained from ATCC 14891, were inoculated into 20 flasks (500-mL Erlenmeyers each containing 100 mL of medium). Incubation was at 28 °C on a rotary shaker (225 rpm) for 6 days. After harvesting, whole broth (2 L) was stirred for 2 h with XAD-2 polystyrene resin, collected by filtration, washed with water (1 L), and eluted with methanol (1 L). This methanol eluate was concentrated to dryness and then triturated with ethyl acetate (3 times, 500 mL). The ethyl acetate triturates were combined, concentrated to dryness, and partitioned between chloroform/methanol/water (100 mL of each). The lower layer from this partition was concentrated to dryness and subjected to countercurrent chromatography on an Ito multilayered coil planet centrifuge in a solvent system of hexane/ethyl acetate/methanol/water (70:30:15:6) with the lower layer as stationary. The isolation of [U-^{13}C]ascomycin was followed throughout by measuring the activity against *Aspergillus niger* in a standard agar disc diffusion assay. The *Aspergillus niger* active material eluted after approximately one column volume to yield ~40 mg of pure [U-^{13}C]ascomycin.

Sample Preparation. Recombinant human FKBP was cloned from a Jurkat T-cell cDNA library and expressed in *Escherichia coli* using the pKK233-2 vector containing a trc promoter as previously described.[10] FKBP was isolated from these cells using ion exchange and size exclusion chromatography.[10] The NMR sample was prepared by exchanging the protein into a ^2H_2O solution (pH = 6.5) containing potassium phosphate (50 mM), sodium chloride (100 mM), and dithiothreitol-d_{10} (5 mM) and concentrating the solution to ~500 μL using a Centricon-10 microconcentrator. The final FKBP concentration was ~3 mM. The [U-^{13}C]ascomycin/FKBP complex was prepared by incubating 1.5 mol equiv of [U-^{13}C]ascomycin with the concentrated protein solution overnight. Excess [U-^{13}C]ascomycin was removed by centrifugation.

NMR. All NMR spectra were acquired on a Bruker AMX600 (600 MHz) spectrometer at 30 °C. The spectra were processed on either a Silicon Graphics 4D/220GTX computer or on a Silicon Graphics 4D/25 computer using in-house written software.

The HMQC spectrum was collected as previously described,[11,12] with a sweep width of 21 739 Hz in ω_1 and 10 000 Hz in ω_2. A total of 160 complex t_1 points were collected with 32 scans per t_1 point. The ^{13}C-COSY experiment was collected in the phase-sensitive mode[13] with a sweep width of 31 250 Hz in both ω_1 and ω_2. Proton decoupling was employed during the entire experiment with reduced power during the relaxation delay between scans to avoid

(3) Liu, J.; Farmer, J. D., Jr.; Lane, W. S.; Friedman, J.; Weissm, S. L.; Schreiber, S. L. Calcineurin is a common target of cyclophilin-cyclosporin A and FKBP-FK-506 complexes. *Cell* **1991**, *66*, 807–815.
(4) Arai, T.; Koyama, Y.; Suenaga, T.; Honda, H. Ascomycin, an antifungal antibiotic. *J. Antibiot.* **1962**, *15*, 231–232.
(5) Hatanka, H.; Kino, T.; Miyata, S.; Inamura, N.; Kuroka, A.; Goto, T.; Tanaka, H.; Okuhara, M. FR-900520 and FR-900523, novel immunosuppressants isolated from a Sreptomyces. II. Fermentation, isolation and physico-chemical and biological characteristics. *J. Antibiot.* **1988**, *41*, 1592–1601.
(6) Petros, A. M.; Gampe, R. T., Jr.; Gemmecker, G.; Neri, P.; Holzman, T. F.; Edalji, R.; Hochlowski, J.; Jackson, M.; McAlpine, J.; Luly, J. R.; Pilot-Matias, T.; Pratt, S.; Fesik, S. W. NMR studies of an FK-506 analog, [U-^{13}C]ascomycin, bound to FKBP: conformation and regions of ascomycin involved in binding. *J. Med. Chem.* **1991**, *34*, 2925–2928.
(7) Van Duyne, G. D.; Standaert, R. F.; Karplus, P. A.; Schreiber, S. L.; Clardy, J. Atomic structure of FKBP-FK-506, an imunnophilin-imunnosuppressant complex. *Science* **1991**, *252*, 839–842.
(8) Karuso, P.; Kessler, H.; Mierke, D. F. Solution structure of FK-506 from nuclear magnetic resonance and molecular dynamics. *J. Am. Chem. Soc.* **1990**, *112*, 9434–9436.
(9) Mierke, D. F.; Schmieder, P.; Karuso, P; Kessler, H. Conformational analysis of the cis- and trans-Isomers of FK-506 by NMR and molecular dynamics. *Helv. Chim. Acta.* **1991**, *74*, 1027–1047.
(10) Edalji, R.; Pilot-Matias, T. J.; Pratt, S. D.; Egan, D. A.; Severin, J. M.; Gubbins, E. G.; Smith, H.; Park, C. H.; Petros, A. M.; Fesik, S. W.; Luly, J.; Burres, N. S.; Holzman, T. F. Characterization of a high expression fusion construct of recombinant human FK-binding protein and comparison to non-fusion recombinant human and natural mammalian FK-binding proteins. *J. Protein Chem.*, in press.
(11) Müller, L. Sensitivity enhanced detection of weak nuclei using heteronuclear multiple quantum coherence. *J. Am. Chem. Soc.* **1979**, *101*, 4481–4484.
(12) Bax, A.; Griffey, R. H.; Hawkins, B. L. Correlation of proton and nitrogen-15 chemical shifts by multiple quantum NMR. *J. Magn. Reson.* **1983**, *55*, 301–315.
(13) Marion, D.; Ikura, M.; Tschudin, R.; Bax, A. Rapid recording of 2D NMR spectra without phase cycling. Application to the study of hydrogen exchange in proteins. *J. Magn. Reson.* **1989**, *85*, 393–399.

excessive sample heating. A 3D HMQC-NOESY experiment[14] was acquired with a mixing time of 40 ms. The spectrum consisted of $40(t_1) \times 64(t_2) \times 2048(t_3)$ complex points with a spectral width of 6494 Hz (folded) in ω_1 and 5000 Hz in ω_2 and ω_3. The initial delay in the t_1 dimension was set to exactly half of the dwell time so that the folded peaks were 180° out of phase with respect to the unfolded peaks.[15]

Structure Calculations. Three-dimensional structures were calculated using a hybrid distance geometry/dynamical simulated annealing approach.[16-18] The DSPACE distance geometry algorithm (Hare Research, Inc.) was used to generate 200 initial structure which were subsequently refined with a dynamical simulated annealing protocol using the XPLOR program.[19] The protocol consisted of 50 steps of Powell minimization followed by 4 ps of molecular dynamics at 1000 K (timestep of 2 fs) using the F_{repel} function[18] for the van der Waals repulsive term with a force constant of 0.002 kcal mol^{-1} Å^{-2}. NOE constraints were introduced at this stage using a soft-square-well potential with an asymptote slope of 0.1 and with a value of 0.5 Å for the transition from the square-well to asymptote function. The NOE force constant was 50 kcal mol^{-1} Å^{-2}. In the next stage, the asymptote slope was stepwise increased by adding 0.1 to the previous slope to a final value of 1.0. Concomitantly, the van der Waals force constant was increased by multiplying the previous value by 1.5 until a final value of 0.1 was obtained. Each step consisted of 1 ps of restrained molecular dynamics at 1000 K (timestep of 2 fs). This stage was then followed by slow cooling from 1000 K to 300 K in steps of 25 K. During this cooling each step consisted of 0.15 ps restrained molecular dynamics (timestep of 2 fs) with a square-well NOE potential, van der Waals force constant of 4 kcal mol^{-1} Å^{-2}, and van der Waals radii of 0.8 times the value used in CHARMM[20] for F_{repel}. In the last stage, the structures were subjected to 500 steps of Powell restrained energy minimization.

The proton-proton distances used as constraints in the structure calculations were obtained from the NOE cross-peak volumes measured from the 3D NOE spectrum acquired at a mixing time of 40 ms. The distances were calculated using the known fixed distance of 1.79 Å between methylene protons as a ruler. A total of 88 proton-proton distances were used in the structure calculations with upper and lower bounds of ±20% of the calculated distance. For the distances involving methyl groups, 0.5 Å was added to the calculated distance to correct for the pseudo atom. In addition to these constraints, three lower bound constraints were added based on the lack of observable NOEs.

Results and Discussion

NMR Assignments. The ^{1}H and ^{13}C NMR signals were assigned from an analysis of two-dimensional ^{1}H/^{13}C and ^{13}C/^{13}C correlation experiments and NOE data. From the one-bond carbon–carbon correlations observed in a ^{13}C COSY spectrum of [U-^{13}C]ascomycin bound to FKBP, it was possible to assign all of the ^{13}C resonances with the exception of the carbons from the three methoxy groups. Once the carbon resonances had been assigned, their attached protons were assigned via the one bond ^{13}C/^{1}H coupling in an HMQC experiment (Figure 2). The only unassigned signals were those from the three methoxy

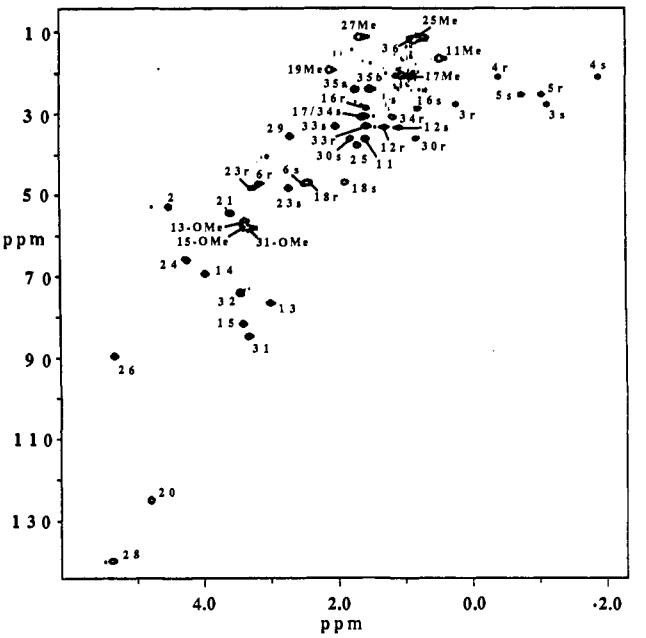

Figure 2. HMQC spectrum of [U-^{13}C]ascomycin bound to FKBP (ω_1, vertical axis, ^{13}C; ω_2, horizontal axis, ^{1}H).

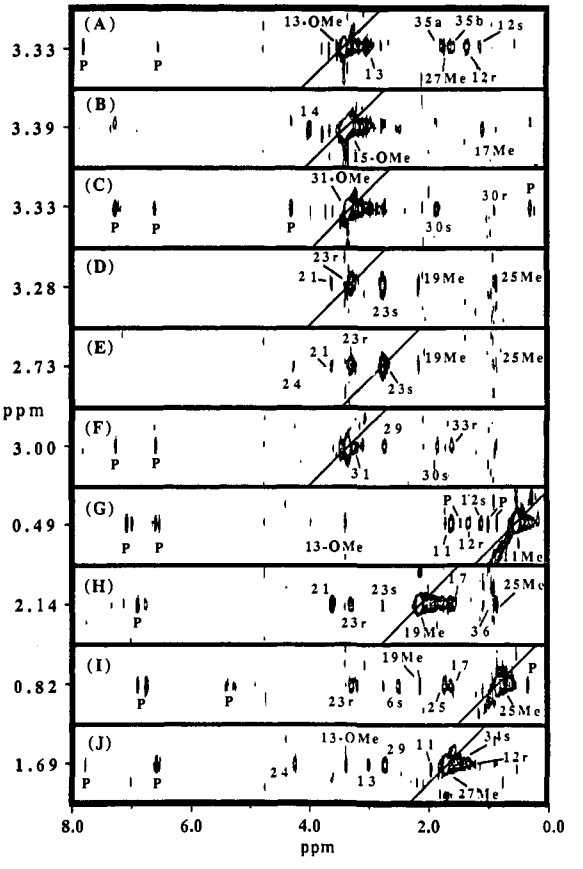

Figure 3. (A–E) Cross sections (ω_2, vertical axis; ω_3 horizontal axis) from a 3D ^{13}C HMQC-NOESY spectrum of [U-^{13}C]ascomycin bound to FKBP at the ^{13}C chemical shifts (ω_1): (A) 56.8, (B) 57.5, (C) 58.2, (D) 48.1, (E) 48.1, (F) 84.5, (G) 16.5, (H) 19.2, (I) 11.3 and (J) 11.3 ppm. The diagonal peaks are indicated in each of the planes by a solid line and crosspeaks labeled with a "P" are NOEs observed from the ligand to the protein.

(14) Fesik, S. W.; Zuiderweg, E. R. P. Heteronuclear three-dimensional NMR spectroscopy. A strategy for the simplication of homonuclear two-dimensional NMR spectra. *J. Magn. Reson.* **1988**, *78*, 588–593.
(15) Kay, L. E.; Marion, D.; Bax, A. Practical aspects of 3D heteronuclear NMR of proteins. *J. Magn. Reson.* **1989**, *84*, 72–84.
(16) Clore, G. M.; Appella, E.; Yamada, M.; Matsushima, K.; Gronenborn, A. M. Three-dimensional structure of interleukin 8 in solution. *Biochemistry* **1990**, *29*, 1689–1696.
(17) Holak, T. A.; Nilges, M.; Oschkinat, H. Improved strategies for the determination of protein structures from NMR data: the solution structure of acyl carrier protein. *FEBS Lett.* **1989**, *242*, 218–224.
(18) Nilges, M.; Clore, M.; Gronenborn, A. M. Determination of three-dimensional structures of proteins from interproton distance data by dynamical simulated annealing from a random array of atoms. *FEBS Lett.* **1988**, *239*, 129–136.
(19) Brünger, A. T. XPLOR Manual, version 2.1., 1990.
(20) Brooks, B. R.; Bruccoleri, R. E.; Olafson, B. D.; States, D. J.; Swaminathan, S.; Karplus, M. CHARMM: A program for Macromolecular energy, minimization, and dynamics calculations. *J. Comput. Chem.* **1983**, *4*, 187–93.

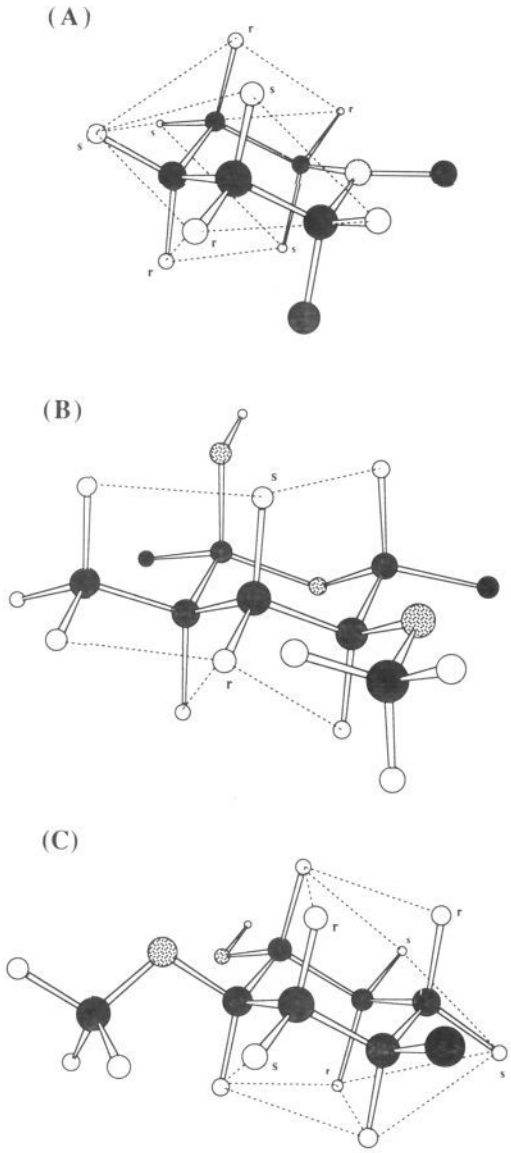

Figure 4. Schematic illustration of the NOEs observed within the (A) piperidine, (B) pyranose, and (C) cyclohexyl rings of [U-^{13}C]ascomycin bound to FKBP. Protons are represented by open circles and NOEs by dashed lines.

groups of the ascomycin. These resonances were assigned from the NOEs observed in the 3D HMQC-NOESY spectrum. Figure 3, parts A, B, and C, depict ω1 slices extracted from the 3D HMQC-NOESY spectrum at the carbon chemical shifts of the three methoxy carbons. NOEs were observed from 13-OMe to 13, 12*R* and 12*S*, from 15-OMe to 14 and 17Me, and from 31-OMe to 30*R* and 30*S*. Although 13-OMe and 31-OMe protons have identical chemical shifts, the sets of NOEs involving these two methoxy groups were easily resolved in the heteronuclear 3D NOE experiment by editing with respect to their different ^{13}C chemical shifts.

All methylene protons of ascomycin were sterospecifically assigned (except those of the ethyl side chain) using a combination of approaches. The protons attached to carbons 3, 4, 5, and 6 of the piperdine ring were assigned as either *pro-R* or *pro-S* based on NOEs observed in the 3D HMQC-NOESY experiment. Figure 4A schematically illustrates the NOEs observed between these ring protons. From this pattern of NOEs, all eight methylene protons could be stereospecifically assigned and it could be shown

Table I. Structural Statistics and Atomic rms Differences for [U-^{13}C]Ascomycin Bound to FKBP

(A) Structural Statistics

	SA_i	AV	AV_m
rms Deviation from Distance Constraints (Å)[a]			
	0.0263 ± 0.0015	0.11	0.027
rms Deviation from Idealized Geometry			
bonds (Å)	0.0093 ± 0.0004	0.349	0.0090
angles (deg)	2.81 ± 0.066	32.51	2.87
impropers (deg)	0.64 ± 0.04	0.77	0.63
Conformational Energy			
E_{NOE} (kcal/mol)[b]	1.89 ± 0.21	32.41	1.96
E_{repel} (kcal/mol)[c]	3.14 ± 0.26	247.53	3.31
E_{L-J} (kcal/mol)[d]	−7.00 ± 1.24	189.32	−6.23

(B) Atomic rms Differences for All Heavy Atoms

SA_i vs AV	0.45 ± 0.17
SA_i vs AV_m	0.59 ± 0.19
AV vs AV_m	0.38

[a] SA_i is the average over the final 73 structures; AV is the average structure; AV_m is the structure obtained after restrained energy minimization of AV. [b] E_{NOE} is the energy contribution from the square-well NOE potential using a force constant of 50 kcal/mol·Å^2. [c] E_{repel} is the van der Waals repulsion energy term calculated with the F_{repel} potential and a force constant of 4 kcal·mol^{-1}·Å^{-2} and a hard-sphere van der Waals radii 0.8 times the CHARMM (ref 20) function. [d] E_{L-J} is the Lennard-Jones van der Waals energy calculated using the CHARMM function.

that the piperidine ring adopts a chair conformation. The same approach was used to stereospecifically assign the methylene protons of the pyranose and cyclohexyl rings. The key NOEs used to make these assignments are illustrated in Figure 4, parts B and C. The remaining methylene protons, at positions 16, 18, and 23, were stereospecifically assigned using an approach[17,21] in which the chirality of prochiral pairs is initially allowed to "float" between *pro-R* and *pro-S* during the simulated annealing stage of the structure calculation. If the NOE data is sufficient to define the stereochemistry at a particular site, one of the possible prochiral assignments will be statistically favored. For the methylene protons at positions 16, 18, and 23, nearly all of the low energy structures that satisfied the NOE-derived distance constraints maintained the same stereochemistry, defining the stereochemistry at these sites.

Bound Conformation of Ascomycin. Of the 200 initial structures generated from the DSPACE program that were further refined with dynamical simulated annealing using XPLOR, 73 were chosen that best satisfied the NOE constraints. All of these structures satisfied every distance constraint to within 0.2 Å. In addition, the structures have relatively minor deviations from idealized geometry as is shown in Table I. For these 73 structures, the average rms deviation of all heavy atoms from a calculated average structure was 0.45 ± 0.17 Å. Use of a 2-fold dihedral angle term during the molecular dynamics and simulated annealing steps allowed transitions between the cis and trans conformations for the amide bond. The lowest energy structure obtained using this approach contained a trans 7,8 amide bond. Furthermore, within 10 kcal/mol of this lowest energy structure, only two structures were obtained that contained a cis amide bond whereas; 33 were obtained with a trans amide bond.

Many of the NOEs which were most important in determining the overall structure of the bound ascomycin are

(21) Weber, P. L.; Morrison, R.; Hare, D. J. Determining Stereospecific ^{1}H nuclear magnetic resonance assignments from distance geometry calculations. *J. Mol. Biol.* **1988**, *204*, 483–487.

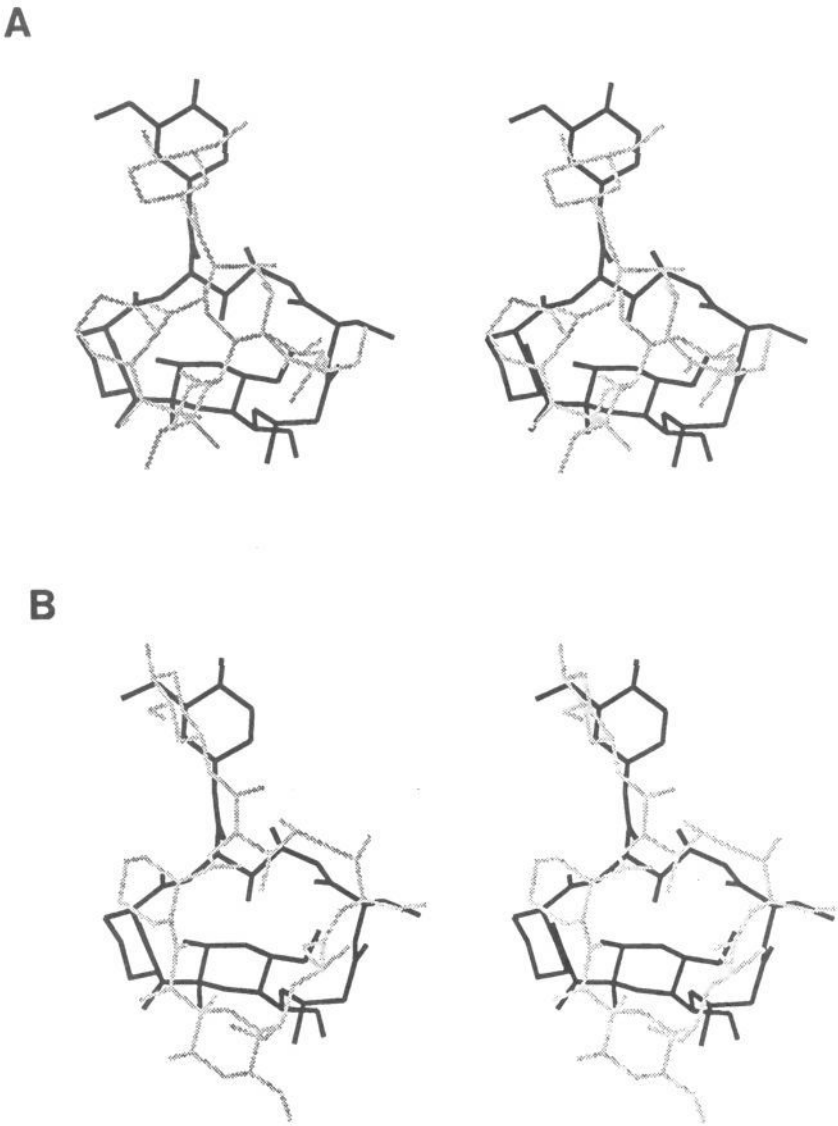

Figure 5. Stereoviews of the superposition on the common heavy atoms of the average NMR structure of bound ascomycin (bold) on the NMR-derived structures of free FK-506 in chloroform solution. (A) Major conformer (66%) with a cis-7,8 amide bond, rms deviation = 3.46 Å. (B) Minor conformer (33%) with a trans-7,8 amide bond, rms deviation = 3.22 Å.

shown in Figure 3, panels F–J. NOEs from proton 31 (Figure 3F) to 29 and 33*R* helped to constrain the cyclohexyl ring of ascomycin to a chair conformation with the methoxy group in an equitorial position. Likewise, NOEs from 11Me (Figure 3G) to both 12*R* and 12*S*, and to 13-OMe determined the conformation of the pyranose ring, and NOEs from 27Me to protons 11, 12*R*, and 13 (Figure 3J) oriented the pyranose ring with respect to the rest of the macrocycle. The relative orientation of the piperidine ring with respect to the rest of the macrocycle was characterized by an NOE from 6S to 25Me (Figure 3I). Finally, a turn in the 19–25 region of ascomycin was defined by NOEs from 19Me to 21, 23*R*, 23*S*, and 25Me (Figure 3H).

As described in our earlier communication,[6] the conformation of ascomycin when bound to FKBP was found to be very different than the X-ray structure of uncomplexed FK-506, but more closely resembled the X-ray structure of rapamycin. Recently, the three-dimensional structure of FK-506 was determined in solution by NMR.[8,9] Figure 5 shows a superposition of ascomycin (dark line) on the two, cis 7,8 (Figure 5A) and trans 7,8 (Figure 5B), forms of free FK-506 observed in chloroform solution. Since ascomycin binds to FKBP in a single conformation containing a trans 7,8 amide bond, one might expect the bound conformation of ascomycin to resemble the trans 7,8 form of FK-506 in solution. However, it is clear from Figure 5 that the bound conformation of ascomycin is very different from either the major (cis) or minor (trans) form of free FK-506. Thus, the conformation of ascomycin when bound to FKBP was found to be quite different from the structure of uncomplexed FK-506 determined either in solution or in the solid state. However, as shown in Figure 6, the conformation of FK-506 and ascomycin when bound to FKBP determined in the solid state by X-ray crystallography[7] or in solution by NMR were essentially identical (rmsd of 0.56 Å).

FKBP/Ascomycin NOEs. In our earlier communication[6] we identified several FKBP/ascomycin NOEs. From this data, we were able to determine those portions of ascomycin that were in close proximity to FKBP. However, since the FKBP protons were not assigned, we were unable to determine at that time which amino acid residues of FKBP were involved in binding to ascomycin. Recently, we have completely assigned the ^{1}H, ^{13}C, and ^{15}N resonances of the FKBP/ascomycin complex from a series of heteronuclear double and triple resonance 3D and 4D

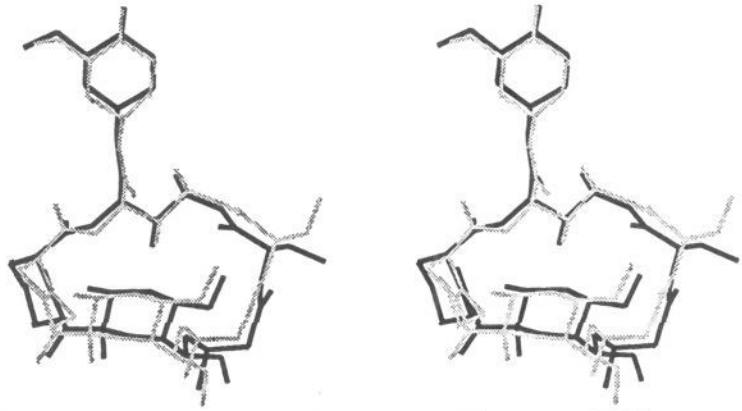

Figure 6. Stereoview of the superposition on the common heavy atoms of the average NMR structure of bound ascomycin (bold) on the X-ray crystal structure of FK-506 bound to FKBP, rms deviation = 0.56 Å.

NMR experiments.[22] From these assignments, the previously observed FKBP/ascomycin NOEs could now be assigned. A list of these NOEs appears in Table II. Also shown in Table II is a comparison of the distances derived from the FKBP/ascomycin NOEs to intermolecular proton–proton distances measured from the X-ray crystal structure of the FKBP/FK-506 complex.[7] For the most part the intermolecular proton–proton distances determined by NMR match closely those measured in the X-ray structure. However, there are some exceptions which involve the Y82, H87, and I90 side chains of FKBP. These are denoted in Table II with an asterisk. Examination of 3D and 4D NOESY data collected on [U-^{13}C,^{15}N]FKBP bound to ascomycin (unpublished data) shows that the conformation of these side chains in solution may be somewhat different from that observed in the crystal. This is not that surprising since all three side chains are located on the surface of the protein and may have some conformational flexibility in solution. A detailed comparison of the solution structure of the FKBP/ascomycin complex and the X-ray structure of the FKBP/FK-506 complex is in progress.

Conclusions

We have used heteronuclear three-dimensional NMR techniques to determine the conformation of a ^{13}C-labeled ligand bound to its target protein. In addition, we have identified and have assigned several FKBP/ascomycin NOEs which help define the structure of the binding pocket. The approach that we have used for determining the conformation of an enzyme-bound ligand is very general in nature and can be applied to virtually any system in which a ligand is tightly bound to a protein. It has been previously used to determine the structure of another immunosuppressant, cyclosporin A, when bound to its target protein, cyclophilin.[23-25] An advantage of this approach is that the time required for data aquisition and analysis is relatively short, especially when compared to the time required for a complete structure determination of an enzyme–ligand complex. Furthermore, since we are ac-

Table II. Proton–Proton Distances Estimated from FKBP/Ascomycin NOEs Compared to Intermolecular Proton–Proton Distances Measured from an X-ray Crystal Structure of the FKBP/FK-506 Complex

	distances (Å)	
FKBP/ascomycin protons[a]	from NOE data	from X-ray
V55 H$^{\beta}$/3*R*	2.0–3.0	2.6
I56 H$^{\gamma 1,2}$/3*R*	2.2–3.4	2.5
F46 H$^{\epsilon}$/4*S*	3.6–5.4	4.1
W59 H$^{\delta 1}$/4*S*	2.3–3.5	3.4
F36 H$^{\delta}$/11-Me	3.8–5.6	5.5
F36 H$^{\epsilon}$/11-Me	3.3–4.9	4.2
Y82 H$^{\epsilon}$/11-Me	3.7–5.5	4.2
H87 H$^{\delta 2}$/11-Me	2.7–4.1	4.1
I90 H$^{\beta}$/11-Me	3.0–4.4	4.1
I90 H$^{\delta}$/11-Me*	3.3–4.9	6.6
I91 H$^{\delta}$/11-Me	2.8–4.2	3.1
I90 H$^{\delta}$/12*S**	2.6–3.8	6.0
I90 H$^{\delta}$/12*R**	2.7–4.1	7.3
H87 H$^{\delta 2}$/13-OMe*	2.9–4.3	6.5
H87 H$^{\epsilon 1}$/13-OMe	2.6–3.8	3.5
Y26 H$^{\epsilon 2}$/17-Me	2.6–4.0	3.9
F46 H$^{\delta}$/17-Me	3.2–4.8	4.5
F46 H$^{\epsilon}$/17-Me	3.5–5.3	5.1
F46 H$^{\epsilon}$/17	2.9–4.3	3.9
F46 H$^{\epsilon}$/19-Me	3.4–5.2	5.2
F46 H$^{\epsilon}$/25-Me	3.4–5.2	3.4
F46 H$^{\zeta}$/25-Me	2.2–3.2	2.7
V55 H$^{\gamma 2}$/25-Me	3.3–4.9	4.6
V55 H$^{\alpha}$/26	2.1–3.1	2.4
V55 H$^{\gamma 2}$/26	3.2–4.8	4.6
Y82 H$^{\epsilon}$/27-Me	3.3–4.9	4.2
H87 H$^{\epsilon 1}$/27-Me	2.8–4.2	3.9
Y82 H$^{\epsilon}$/29*	2.7–4.1	4.6
I56 H$^{\gamma 2}$/30*S*	2.6–4.0	2.9
Y82 H$^{\epsilon}$/30*S*	3.0–4.4	3.7
I56 H$^{\gamma 2}$/31-OMe	3.1–4.7	4.5
Y82 H$^{\alpha}$/31-OMe	2.2–3.4	3.1
Y82 H$^{\delta}$/31-OMe	3.2–4.8	4.8
Y82 H$^{\epsilon}$/31-OMe*	3.7–5.5	5.6
Y82 H$^{\delta}$/31*	3.0–4.4	5.5
Y82 H$^{\epsilon}$/31*	3.0–4.6	5.4

[a] Asterisk denotes that intermolecular proton–proton distances as determined by NMR and the X-ray crystal structure do not match closely.

(22) Xu, R. X., Nettesheim, D., Olejniczak, E. T., Meadows, R., Gemmecker, G., Fesik, S. W. ^{1}H, ^{13}C, and ^{15}N assignments and secondary structure of the FK506 binding protein when bound to ascomycin. *Biopolymers*, submitted for publication.

(23) Fesik, S. W.; Gampe, R. T., Jr.; Holzman, T. F.; Egan, D. A.; Edalji, R.; Luly, J. R.; Simmer, R.; Helfrich, R.; Kishore, V.; Rich, D. H. Isotope-edited NMR of cyclosporin A bound to cyclophilin: Evidence for a trans 9,10 amide bond. *Science* **1990**, *250*, 1406–1409.

(24) Fesik, S. W.; Gampe, R. T., Jr.; Eaton, H. L.; Gemmecker, G.; Olejniczak, E. T.; Neri, P.; Holzman, T. F.; Egan, D. A.; Edalji, R.; Helfrich, R.; Hochlowski, J.; Jackson, M. NMR studies of [U-^{13}C]Cyclosporin A bound to cyclophilin. Bound conformation and portions of cyclosporin involved in binding. *Biochemistry* **1991**, *30*, 6574–6583.

(25) Weber, C.; Wider, G.; von Freyberg, B.; Traber, R.; Braun, W.; Widmer, H.; Wüthrich, K. The NMR structure of cyclosporin A bound to cyclophilin in aqueous solution. *Biochemistry* **1991**, *30*, 6563–6574.

tually observing signals from the bound ligand and not from the enzyme, impurities in the enzyme sample can be tolerated.

The precision of the structure that was determined using this approach was quite high with the average rmsd of all heavy atoms from a calculated average structure of 0.45 ± 0.17 Å for the 73 final structures. Furthermore, the NMR-derived structure of bound ascomycin was found to be virtually identical to the recently determined X-ray crystal structure of FK-506 bound to FKBP.[7] Superposition of the common heavy atoms of the two structures, Figure 6, gives an rmsd of 0.56 Å, a value which is within the standard deviation of the rmsd for the 73 final NMR structures. However, the conformation of ascomycin when bound to FKBP was found to be quite different from the conformation of the free ligand either in solution or in the solid state. These results are similar to those obtained for cyclosporin A (CsA) in which the conformation of CsA when bound to cyclophilin was found to be very different from the conformation of free CsA.[23-25] Thus, the three-dimensional structure of the uncomplexed molecule may not be a suitable template for designing new molecules and may be inappropriate for rationalizing structure–activity relationships.

Acknowledgment. We thank J. Hochlowski and M. Jackson for [U-^{13}C]ascomycin, T. Holzman for FKBP, and G.W. Carter and T.J. Perun for their support and encouragement. P. Neri acknowledges support from a fellowship from the CNR, Italy (Bando No. 203.03.22, Com. Scienze Chimiche). We also thank Prof. Horst Kessler, Technische Universität München, for providing us with the coordinates of the two forms of FK-506 in chloroform solution.

"Mixed Inhibitor–Prodrug" as a New Approach toward Systemically Active Inhibitors of Enkephalin-Degrading Enzymes

Marie-Claude Fournié-Zaluski, Pascal Coric, Serge Turcaud, Evelyne Lucas, Florence Noble, Raphael Maldonado, and Bernard P. Roques*

Université René Descartes, UFR des Sciences Pharmaceutiques et Biologiques, Département de Chimie Organique, U266 INSERM—URA498 CNRS, 4, Avenue de l'Observatoire, 75270 Paris Cedex 06. *Received December 9, 1991*

In order to evaluate the possible advantages of potentiating the effects of the endogenous enkephalins, to obtain analgesia without the serious drawbacks of morphine, it was essential to design systemically active compounds which inhibit the two metabolizing enzymes, aminopeptidase N (APN) and neutral endopeptidase 24.11 (NEP). A new concept combining the idea of "prodrug" and "mixed inhibitor" was therefore developed. Given the high efficiency of β-mercaptoalkylamines as APN inhibitors and of *N*-(mercaptoacyl) amino acids as NEP inhibitors, compounds associating these molecules through disulfide or thioester bonds, which are known to increase lipophilicity and to favor passage across the blood–brain barrier, have been synthesized. An HPLC study indicated that the disulfide bridge was resistant to serum enzymes but was cleaved by brain membrane homogenates, suggesting that the active inhibitors were released in the central nervous system. The validity of the approach was verified by the efficient antinociceptive responses obtained in the hot plate test in mice after iv administration of disulfide-containing inhibitors (ED_{50}s of from 4 to 26 mg/kg on the jump latency time). The analgesic potencies of the "mixed inhibitor–prodrug" RB 101 [$H_2NCH(CH_2CH_2SCH_3)CH_2SSCH_2CH(CH_2Ph)CONHCH(CH_2Ph)COOCH_2Ph$] after iv administration were three times greater than those of a similar combined dose of its two constitutive moieties. The separation of the two diastereoisomers constituting RB 101 showed that the analgesia has a stereochemical dependence, the (*S,S,S*)-isomer being more active than the (*S,R,S*)-isomer. Furthermore, in the tail flick test in the rat, RB 101 gave 38% analgesia at a dose of 80 mg/kg. Due to its high efficiency and its longer pharmacological effect, RB 101 was selected for a complete study of its analgesic properties.

Introduction

The antinociceptive and behavioral responses to various physical or mental stresses evoked by interaction of the endogenous opioid peptides enkephalins with opioid receptors have been shown to be potentiated by protecting the peptides from enzymatic inactivation (review in ref 1). The enkephalins are rapidly hydrolyzed in vivo by two well-defined enzymes, neutral endopeptidase, NEP (EC 3.4.24.11), and aminopeptidase N, APN (EC 3.4.11.2). Inhibition of only one of these enzymes, NEP, by thiorphan[2] or SCH 32615,[3] or APN, by bestatin,[4] does not increase the endogenous enkephalin concentration to a level sufficient to induce strong analgesic responses, even after icv administration. To overcome this problem, we have developed the concept of mixed inhibitors, i.e. molecules able to inhibit both enzymes. Among these compounds, hydroxamate-containing inhibitors, such as kelatorphan[5] and especially RB38A,[6] were shown to produce, after icv administration, naloxone-reversible antinociceptive re-

* Author to whom correspondence should be addressed.

(1) Roques, B. P.; Fournié-Zaluski, M. C. Enkephalin degrading enzyme inhibitors: A physiological way to new analgesics and psychoactive agents. *NIDA Res. Monogr.* **1986**, *70*, 128–154.
(2) Roques, B. P.; Fournié-Zaluski, M. C.; Soroca, E.; Lecomte, J. M.; Malfroy, B.; Llorens, C.; Schwartz, J. C. The enkephalin inhibitor thiorphan shows antinociceptive activity in mice. *Nature* **1980**, *288*, 286–288.
(3) Chipkin, R. E.; Berger, J. G.; Billard, W.; Iorio, L. C.; Chapman, R.; Barnett, A. Pharmacology of SCH 34826, an orally active enkephalinase inhibitor analgesic. *J. Pharmacol. Exp. Ther.* **1988**, *245*, 829–838.
(4) Carenzi, A.; Frigeni, V.; Della Bella, D. Strong analgesic activity of Leu enkephalin after inhibition of brain aminopeptidase: A pharmacological study. *Advances in endogenous and exogenous opioids. Proceedings of the International Narcotic Research Conference*; Kyoto; Takagi, H., Simon, E. J., Eds.; Elsevier Biomedical Press, Amsterdam, 1981; pp 267–269.

0022-2623/92/1835-2473$03.00/0